



**HAL**  
open science

## Pre-yield shearing regimes of magnetorheological fluids

Waad Nassar, Xavier Boutillon, José Lozada

► **To cite this version:**

Waad Nassar, Xavier Boutillon, José Lozada. Pre-yield shearing regimes of magnetorheological fluids. SMASIS2012, Sep 2012, Stone Mountain, United States. pp.1-6, 10.1115/SMASIS2012-8047. hal-04582465

**HAL Id: hal-04582465**

**<https://polytechnique.hal.science/hal-04582465>**

Submitted on 22 May 2024

**HAL** is a multi-disciplinary open access archive for the deposit and dissemination of scientific research documents, whether they are published or not. The documents may come from teaching and research institutions in France or abroad, or from public or private research centers.

L'archive ouverte pluridisciplinaire **HAL**, est destinée au dépôt et à la diffusion de documents scientifiques de niveau recherche, publiés ou non, émanant des établissements d'enseignement et de recherche français ou étrangers, des laboratoires publics ou privés.

# PRE-YIELD SHEARING REGIMES OF MAGNETORHEOLOGICAL FLUIDS

## Waad Nassar

Lab. for the Mechanics of Solids  
Department of Mechanics  
École Polytechnique  
91128 Palaiseau Cedex, France  
and  
CEA, LIST  
Sensorial and Ambient Interfaces Lab.  
91191 Gif-sur-Yvette Cedex, France  
Email: waad.nassar@renault.com

## Xavier Boutillon\*

Lab. for the Mechanics of Solids  
Department of Mechanics  
École Polytechnique  
91128 Palaiseau Cedex, France  
Email: boutillon@lms.polytechnique.fr

## José Lozada

CEA, LIST  
Sensorial and Ambient Interfaces Lab.  
91191 Gif-sur-Yvette Cedex, France  
Email: jose.lozada@cea.fr

## ABSTRACT

*We analyzed experimentally the pre-yield regime of some MRFs. The hearing response is ruled by two successive regimes and limited by an interfacial phenomenon. The initial response is pseudo-elastic and independent from the magnetic field and of the particle volume fraction. The shear-stress limit of this regime is proportional to the square of the magnetic field and to the particle volume fraction. In the next regime, the shear strain is not uniform in the fluid. The increase in average shear stress varies linearly with the increase in average shear strain. The variation coefficient is proportional to the square of the magnetic field and decreases with the particle volume fraction. Finally, a loss of adhesion of the magnetic aggregates with the shearing plate or the magnetic pole occurs. The corresponding shear stress is proportional to the square of the magnetic field and to the particle volume fraction.*

## NOMENCLATURE

$B$  Magnetic field across the sheared section of the fluid.  
 $e$  Thickness of the shearing plate.  
 $g$  Gap containing the MRF between the magnetic poles.  
 $K_1$  Shearing stiffness in the initial regime.

$K_2$  Shearing apparent stiffness in the intermediate regime.  
 $S$  Area of magnetized and sheared portion of the MRF.  
 $x$  Position of the shearing plate.  
 $\gamma$  Shear strain in the fluid.  
 $\Phi$  Volume fraction of magnetic particles.  
 $\tau$  Shear stress in the fluid.  
 $\tau_y$  Yield-stress of the MRF in the Bingham model.  
 $\tau_{12}$  Shear stress limiting the initial regime.  
 $\tau_{23}$  Shear stress initiating the sliding regime.

## INTRODUCTION

Magneto-rheological fluids are suspensions of magnetic micro-particles in a non-magnetic carrier fluid (Fig. 1). They are part of smart fluids of which characteristics vary upon the application of a magnetic field.

At large shear rates, it has been shown [1–3] that the Bingham model is applicable to these fluids. This model, as described in Fig. 2 and by Eqn. 1, predicts a linear dependency between the variations of the shear rate and the variations of the shear stress when the latter exceeds the so-called Bingham threshold (or yield-stress)  $\tau_y$ .

---

\*Address all correspondence to this author.

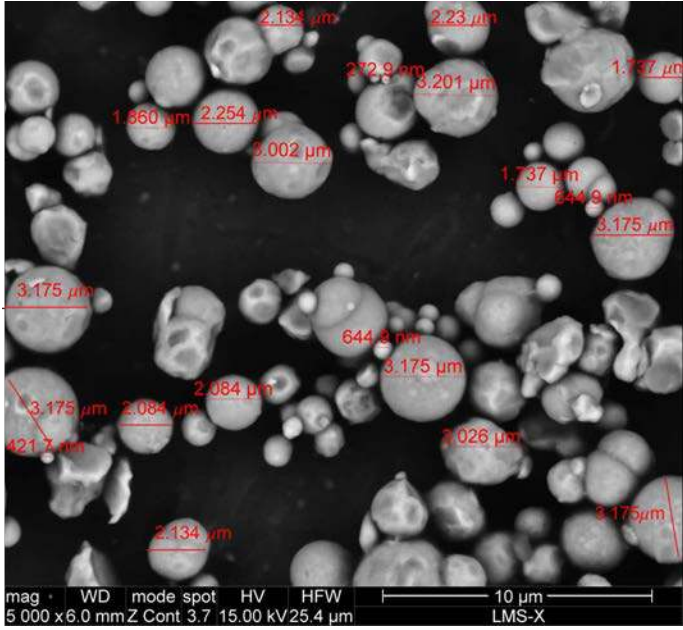


**FIGURE 1.** SCANNING ELECTRONIC MICROSCOPY OF THE SURFACE OF A MRF.

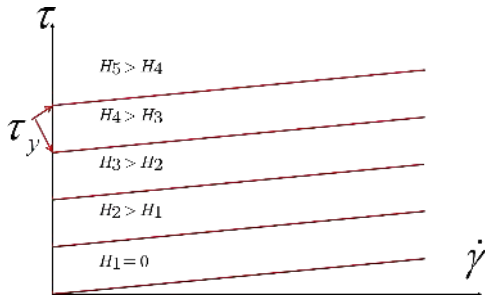


**FIGURE 2.** SHEAR STRESS  $\tau$  AS A FUNCTION OF THE SHEAR RATE  $\dot{\gamma}$  IN THE BINGHAM MODEL (SEE (EQN. 1)) FOR DIFFERENT MAGNETIC FIELDS  $H$ .

$$\begin{cases} \tau = \tau_y(H) + \eta \dot{\gamma} & \tau \geq \tau_y \\ \dot{\gamma} = 0 & \tau < \tau_y \end{cases} \quad (1)$$

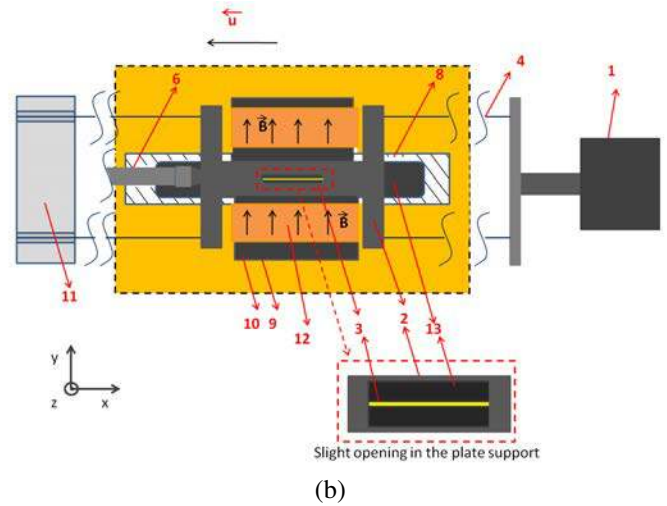
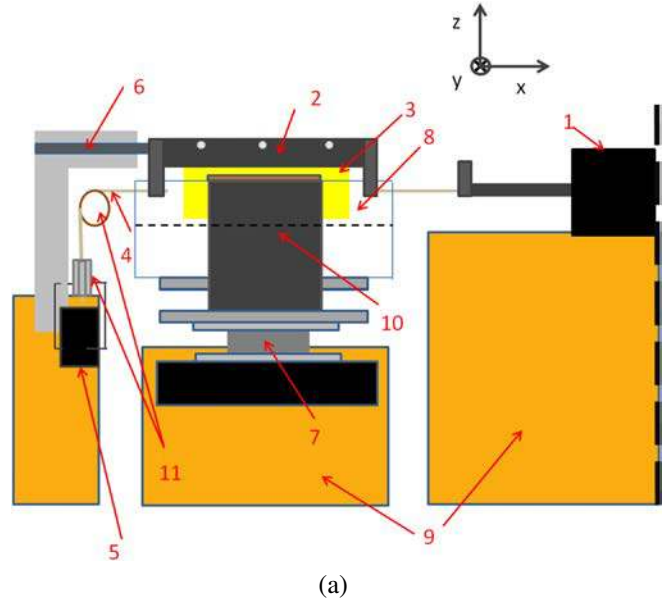
The Bingham model does not say anything below  $\tau_y$  or in a quasi-static shear regime. The behavior of MRFs under such circumstances has received less attention. However, its understanding is needed when the fluid is used in human-machine interfaces since small stresses and shear rates are observed in the transient phases and because these phases are important in this category of applications. This paper is devoted to experimental findings on

MRFs put under small stresses and shear rates.

The MRFs that have been used in this experimental study are provided by the Lord corporation under the commercial references MRF140-CG, MRF132-DG, and MRF122-EG. They denote suspensions with volume fractions  $\Phi$  of 40%, 32%, and 22% respectively, in an hydrocarbon base fluid.

### Experimental setup

The experimental setup is represented in Fig. 3. Some MRF is poured in a relatively small, open cavity. A magnetic field  $B$  is created across the cavity by a magnetic circuit excited by two coils. The dimensions of the gap  $g$  managed across the cavity by the two magnetic poles are  $50 \times 10 \times 1$  mm.



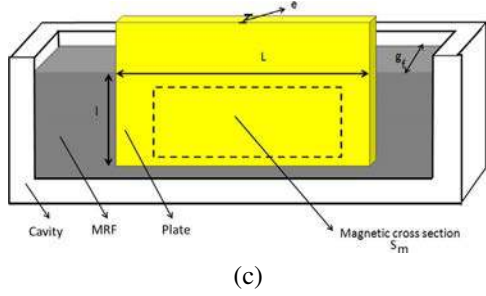


**FIGURE 3.** EXPERIMENTAL SETUP. (a) FRONT VIEW. (b) TOP VIEW. (c) VERTICAL SECTION.

1: STEPPER MOTOR; 2: PLATE HOLDER; 3: SHEARING PLATE; 4: CABLES; 5: EQUILIBRIUM MASS ; 6: DISPLACEMENT SENSOR; 7: FORCE SENSOR; 8: MRF CAVITY; 9: SAND TANK; 10: MAGNETIC CIRCUIT; 11: PULLEYS; 12: COILS; 13: MRF.

The coils are fed by an adjustable current, thus controlling  $B$ . The magnetic circuit has everywhere the same cross-section ( $S = 500 \cdot 10^{-6} \text{ m}^2$ ) so that the magnetic field across the gap can be measured by a probe (Hirst-GM07) inserted in a thin slit of the magnetic circuit, opposite to the gap. The cavity, magnetic circuit, and coils represent a solid which lies on a single three-directional force sensor (Kistler 9251A).

A thin plate with thickness  $e$  (typically 0.3 mm), either in a magnetic or non-magnetic material, is moved in translation along the cavity. The plate area is such that the whole magnetized section of the fluid is sheared by the plate during the motion. There are in fact two separate volumes of the MRF which are sheared, one on each side of the plate. The position of the plate has been adjusted carefully so that the two volumes are equal. The plate velocity  $\dot{x}$  is controlled by a stepper motor. In order to avoid vibration, thin cables have been inserted between the plate and the motor and the different parts of the setup have been installed in separate sand tanks.

The position  $x$  of the plate is measured by a laser sensor (Keyence LB12) so that the shear strain is  $\gamma = \frac{2x}{g-e}$ . Since the motion of the fluid and of its support is null in average, the shearing force  $F$  exerted by the plate on the MRF is the same as the (reaction) force exerted and measured by a three-directional force sensor placed at the base of the cavity. It has been checked that the drag force exerted by the fluid on the plate can be neglected compared to measured forces. It follows that the shear stress is  $\tau = \frac{F}{2S}$ . It has also been checked that the forces in the directions  $y$  and  $z$  can be neglected compared to the component in the  $x$  direction.

All tests have been done at constant speed. When a change in the value of  $B$  was needed, a de-magnetization of the whole magnetic circuit (including the MRF) was done prior to the test.

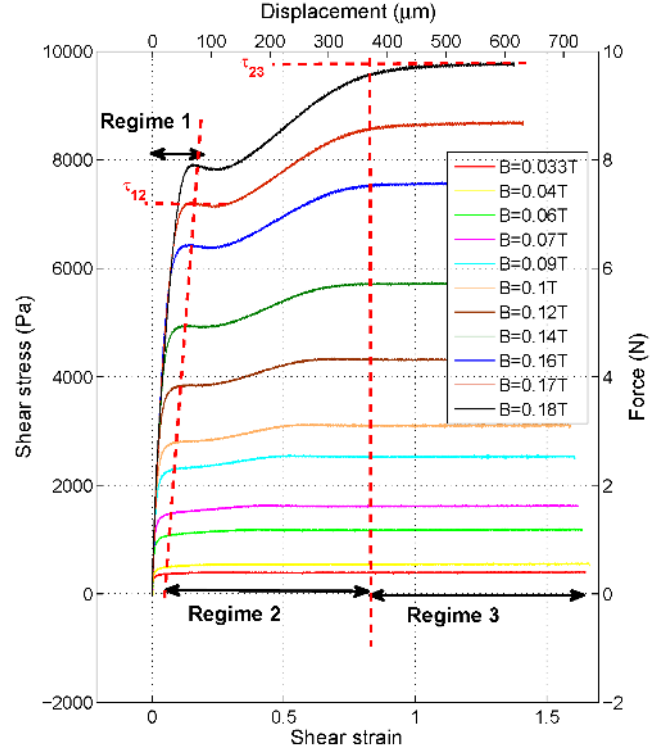


**FIGURE 4.** TYPICAL PRE-YIELD RESPONSE OF A MRF FOR DIFFERENT MAGNETIC FIELDS. SHEAR STRESS  $\tau$  AS A FUNCTION OF THE SHEAR STRAIN  $\gamma$  FOR THE LORD MRF132-DG. THE MAGNETIC FIELD  $B$  RANGES FROM .33 T TO .18 T.

## GENERAL RESULTS

Once magnetized and submitted to a constant shear rate, the fluid very consistently exhibits the behavior shown in Fig. 4. Moreover, as shown in Fig. 5, this behavior does not depend on the shear rate  $\dot{\gamma}$ . Considering this component of shearing only, the MRF in the pre-yield can thus be considered as a pseudo-plastic solid without associated viscosity.

Three regimes can be distinguished in Fig. 4. Initially (Regime 1), the shear stress is a linear function of the shear strain. This regime is limited by the shear stress  $\tau_{12}$  and followed by Regime 2 in which the increase of shear stress  $\Delta\tau$  seems to be proportional to the increase in shear strain  $\Delta\gamma$ . Finally, a limit  $\tau_{23}$  is reached which corresponds to a loss of adhesion between the plate or the MRF.

## INITIAL SHEARING REGIME

The initial regime can be described as a pseudo-elastic regime, thus characterized by a single proportionality coefficient

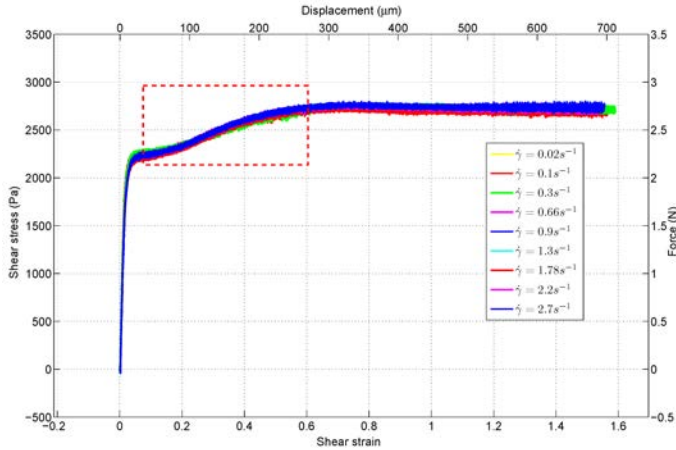


**FIGURE 5.** PRE-YIELD RESPONSES OF A MRF FOR DIFFERENT SHEAR RATES. SHEAR STRESS  $\tau$  AS A FUNCTION OF THE SHEAR STRAIN  $\gamma$  FOR THE LORD MRF122-EG WITH  $B=1$  T. THE SHEAR RATE  $\dot{\gamma}$  RANGES FROM  $.2 \text{ s}^{-1}$  TO  $2.7 \text{ s}^{-1}$ .

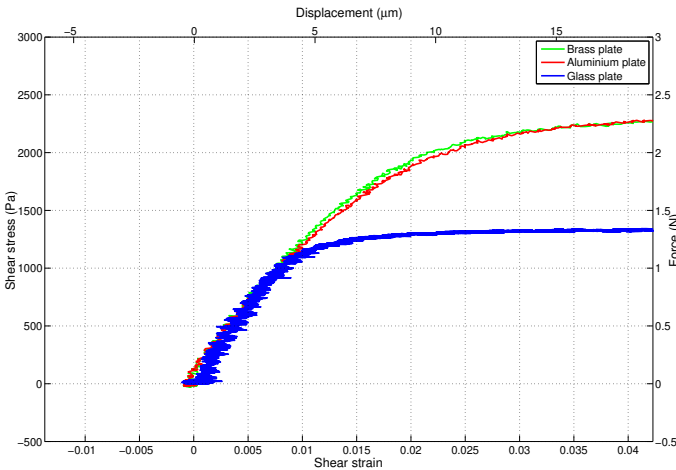


**FIGURE 6.** INITIAL REGIME OF THE PRE-YIELD RESPONSE OF A MRF FOR DIFFERENT MAGNETIC FIELDS. SHEAR STRESS  $\tau$  AS A FUNCTION OF THE SHEAR STRAIN  $\gamma$  FOR THE LORD MRF122-EG.

$K_1$ :

$$\tau = K_1 \gamma \quad (2)$$

According to Fig. 6 and Fig. 7,  $K_1$  does not depend on  $B$  nor on  $\Phi$ . It follows that this regime is controlled by non-magnetic forces. The most natural candidate for explaining the existence of this regime is the necessary present of anti-sedimentation agents in the MRF. Those can be surfactants or polymer coating of the

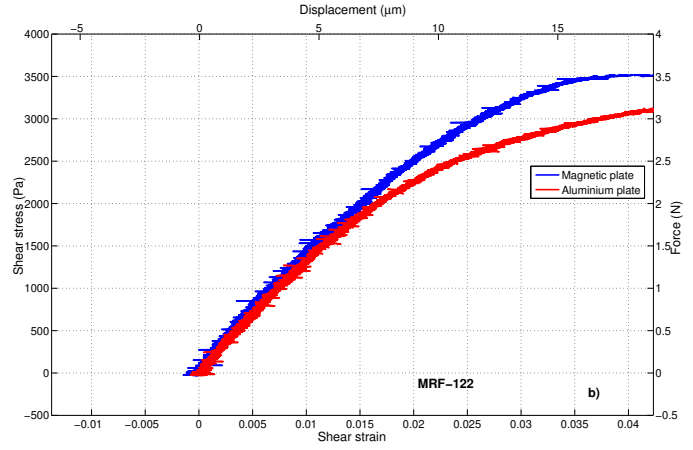


**FIGURE 7.** INITIAL REGIME OF THE PRE-YIELD RESPONSE OF A MRF FOR DIFFERENT MAGNETIC VOLUME FRACTIONS  $\Phi$  OF THE PARTICLES. SHEAR STRESS  $\tau$  AS A FUNCTION OF THE SHEAR STRAIN  $\gamma$  FOR MRF140-CG, MRF132-DG, AND MRF122-EG.

microparticles. Polymer interactions tend to prevent the particle from flowing downwards and thus, introduce a coherence in the material.

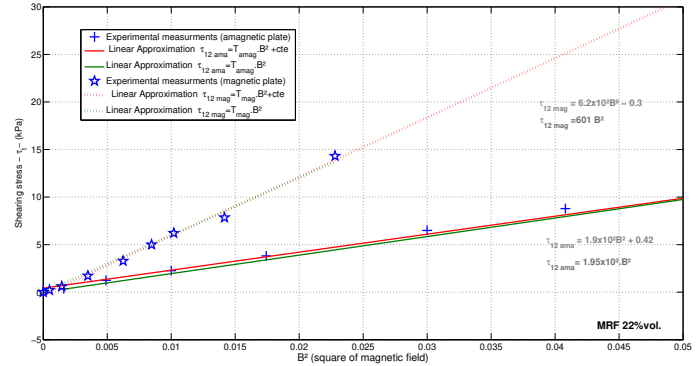


**FIGURE 8.** LIMIT  $\tau_{12}$  OF REGIME 1 AS A FUNCTION OF  $B^2$  FOR THE MRF122-EG. A HIGHER SERIES OF VALUES IS OBTAINED WHEN SHEARING WITH A MAGNETIC PLATE AS COMPARED TO SHEARING WITH A NON-MAGNETIC PLATE.

Regime 1 is limited by the  $\tau_{12}$  threshold. As opposed to  $K_1$ ,  $\tau_{12}$  is proportional to  $B^2$  (see Fig. 8) and may be considered proportional to  $\Phi$  (see Fig. 9). More surprising, this threshold appears to depend strongly on the magnetic or non-magnetic nature of the shearing plate and therefore, cannot be considered as an-

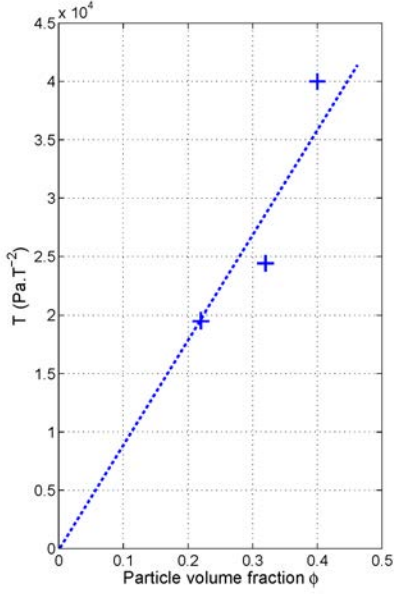


**FIGURE 9.** RATIO  $T = \frac{\tau_{12}}{B^2}$  BETWEEN THE LIMIT STRESS  $\tau_{12}$  OF REGIME 1 AND  $B^2$  AS A FUNCTION OF  $\Phi$ .

trinsic property of the MRF. This might be better understood in view of the nature of Regime 2, as described in the next section.

### INTERMEDIATE SHEARING REGIME

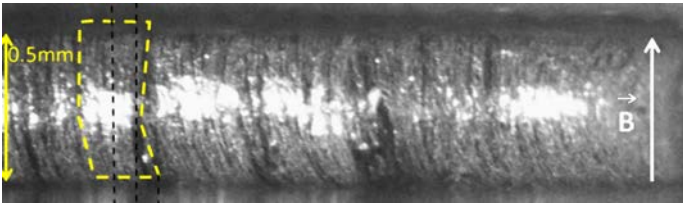


**FIGURE 10.** MICROSCOPIC OBSERVATIONS OF THE MRF STRUCTURE IN REGIME 2. SHEARING WITH A NON-MAGNETIC PLATE,  $B = .1T$ .

A typical configuration of the magnetic aggregates, as observed at the free surface of the MRF, is displayed in Fig. 10. In this regime, aggregates of magnetic particles are *bent* by shearing, instead of being simply tilted. This means that the shear strain is not uniform across the magnetized volume of the MRF. In other words, the MRF sheared between a plate and a magnetic pole cannot be considered as a *material* but rather as a *structure*.

Therefore, it must be expected that the width of the gap and the boundary conditions play a role in the macroscopic behavior of the MRF. Among boundary conditions, we include the nature of the shearing plate, and more generally, the details of the magnetic field configuration at the boundaries.

It appears in Fig. 11 that the variations of the shear stress  $\Delta\tau$  (or possibly, average shear stress  $\langle \Delta\tau \rangle$ ) vary linearly with the average shear strain  $\langle \Delta\gamma \rangle$ . The apparent stiffness  $K_2$ , as defined by (Eqn. 3) is a linear function of  $B^2$ , as shown in Fig. 12. As for  $\tau_{12}$ , the values are larger for a magnetic shearing plate than for a non-magnetic shearing plate.

$$\Delta\tau = K_2 \langle \Delta\gamma \rangle \quad (3)$$

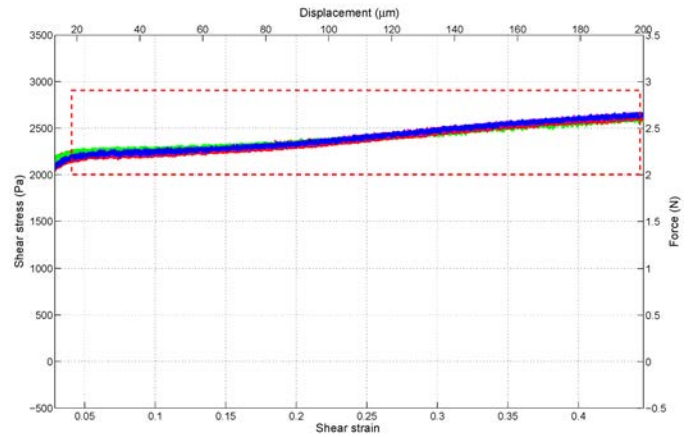


**FIGURE 11.** DETAILED PART OF FIG. 5: SHEAR STRESS AS A FUNCTION OF THE AVERAGE SHEAR STRAIN IN REGIME 2 FOR DIFFERENT SHEARING RATES. SHEARING WITH A NON-MAGNETIC PLATE,  $B = .11T$ .

Finally, the apparent stiffness  $K_2$  is found to decrease with  $\Phi$  (Fig. 13).

### SLIDING REGIME

Above a certain value of  $\tau$ , videos (which will be shown in the conference) of the surface of the MRF make it clear that the plate, when it is non-magnetic, or the magnetic pole in the other case, have lost adhesion with the aggregates of the MRF. This limit value  $\tau_{23}$  is proportional to  $B^2$ , as shown in Fig. 14. At least for a non-magnetic plate, it may also be considered as proportional to  $\Phi$ , as shown in Fig. 15.



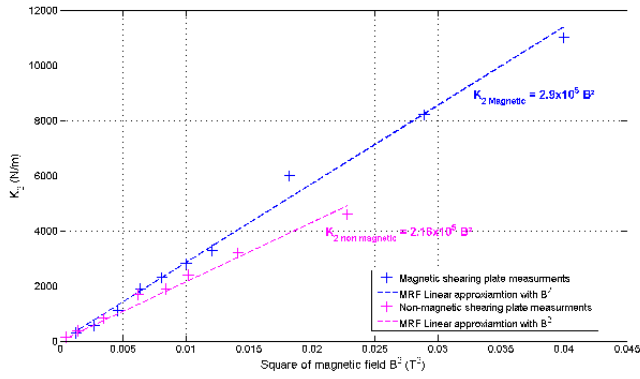


**FIGURE 12.** APPARENT STIFFNESS  $K_2$  BETWEEN  $\Delta\tau$  AND  $\langle \Delta\gamma \rangle$  IN REGIME 2 AS A FUNCTION OF  $B^2$  FOR THE MRF122-EG. A HIGHER SERIES OF VALUES IS OBTAINED WHEN SHEARING WITH A MAGNETIC PLATE AS COMPARED TO SHEARING WITH A NON-MAGNETIC PLATE.

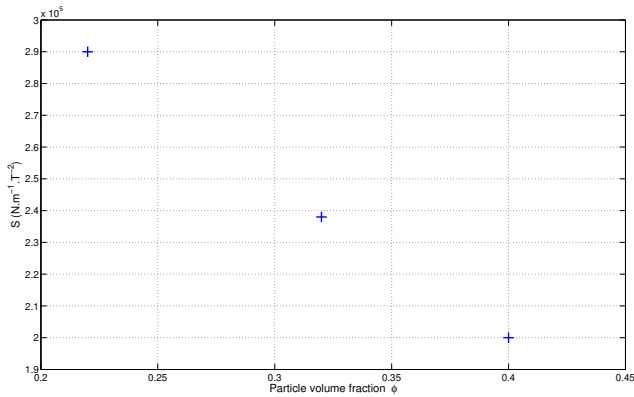


**FIGURE 13.** RATIO  $S = \frac{K_2}{B^2}$  BETWEEN THE APPARENT STIFFNESS  $K_2$  AND  $B^2$  IN REGIME 2 AS A FUNCTION OF  $\Phi$ .

## Conclusion

The experimental findings which have been presented here reveal two well separated pre-yield regimes of a MRF. They lead to attribute a more important role to the non-magnetic interactions between particles than it was thought so far. They also show that shearing of the magnetized aggregates is not always homogeneous in the MRF. This explains why the boundary conditions, at least in small gaps, play a significant role in the shearing strain-stress relationship.

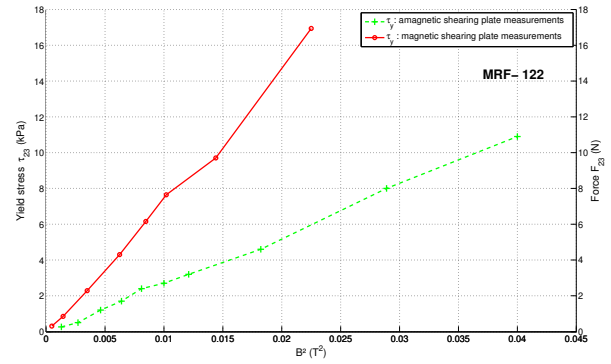


**FIGURE 14.** LIMIT  $\tau_{23}$  OF REGIME 2 AS A FUNCTION OF  $B^2$  FOR THE MRF122-EG. A HIGHER SERIES OF VALUES IS OBTAINED WHEN SHEARING WITH A MAGNETIC PLATE AS COMPARED TO SHEARING WITH A NON-MAGNETIC PLATE.

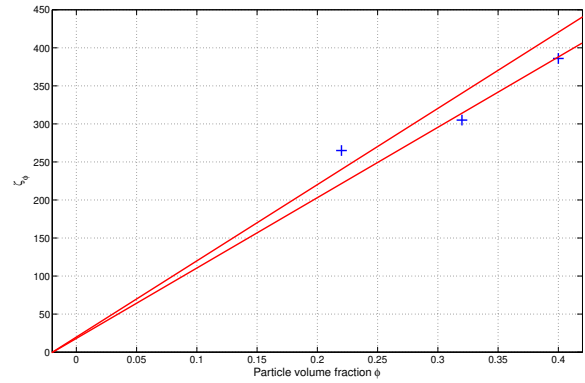


**FIGURE 15.** RATIO  $\zeta = \frac{\tau_{23}}{B^2}$  BETWEEN THE LIMIT STRESS  $\tau_{23}$  OF REGIME 2 AND  $B^2$  AS A FUNCTION OF  $\Phi$ .

## REFERENCES

- [1] Li, W. H., and Zhang, X. Z., 2008. "The effect of friction on magnetorheological fluids". *Korea-Australia Rheology Journal*, **20**(2), June, pp. 45–50.
- [2] Bossis, G., Laci, S., Meunier, A., and Volkova, O., 2002. "Magnetorheological fluids". *Journal Of Magnetism And Magnetic Materials*, **252**(1-3), Nov., pp. 224–228.
- [3] Claracq, J., Sarrazin, J., and Montfort, J. P., 2004. "Viscoelastic properties of magnetorheological fluids". *Rheologica Acta*, **43**(1), Feb., pp. 38–49.